yield of epoxide is dependent upon $[ImH]_i$ (Table VI), but in all cases alkene does not trap all higher valent manganese–oxo species. Examination of Table V shows that at 1.0 M in 2,3-dimethyl-2-butene, *cis*-cyclooctene, cyclohexene, norbornylene, or cyclopentene there is obtained ~80% yields of the corresponding epoxides. The results with TBPH and alkenes suggest the possibility that a portion of DA oxidation occurs within a solvent cage, as previously found for the reaction of $(TPP)Mn^{III}X$ ($X^- = F^-$, Cl^-, Br^-, OCN^-) with NO (see eq 1).[1] Any other explanation based upon a preference for either $1e^-$ oxidation or epoxidation by the imidazole-ligated higher valent manganese–oxo porphyrin species may be discounted, because neither the $1e^-$ oxidizable TBPH nor alkenes are capable of completely trapping the oxo species.

Acknowledgment. This work was supported by a grant from the American Cancer Society and the National Institutes of Health. W.-H.W. expresses appreciation to the Universiti Malaya, Kuala Lumpur, Malaysia, for a sabbatical leave of absence during the tenure of this study. We should like to express appreciation to a referee for helpful comments.

Kinetics and Mechanism of Oxygen Transfer in the Reaction of *p*-Cyano-*N*,*N*-dimethylaniline *N*-Oxide with Metalloporphyrin Salts. 6.[1,2] Oxygen Atom Transfer to and from the Iron(III) C_2cap Porphyrin of Baldwin

Thomas C. Bruice,* C. Michael Dicken, P. N. Balasubramanian, T. C. Woon, and Fu-Lung Lu

Contribution from the Department of Chemistry, University of California at Santa Barbara, Santa Barbara, California 93106. *Received September 19, 1986*

Abstract: The decomposition of *p*-cyano-*N*,*N*-dimethylaniline *N*-oxide (NO) is catalyzed (CH_2Cl_2 solvent at 25 °C) by the SbF_6^- salt of the C_2-capped (*meso*-tetraphenylporphinato)iron(III) of Baldwin ($(TPPC_2cap)Fe^{III}SbF_6$). Since neither NO nor the SbF_6^- anion can fit under the cap, this result establishes that oxygen transfer from NO to the iron(III) center can occur without the intermediate iron(IV)–oxo porphyrin π-cation being hexacoordinated. The products of NO decomposition (*p*-cyano-*N*,*N*-dimethylaniline (DA) 68%, *p*-cyano-*N*-methylaniline (MA) 12%, *p*-cyanoaniline (A) 1%, *N*-formyl-*p*-cyano-*N*-methylaniline (FA) 6%, *N*,*N*'-dimethyl-*N*,*N*'-bis(*p*-cyanophenyl)hydrazine (H) 7%, and CH_2O 3%) account for 100% of the *p*-cyanodimethylaniline moiety of NO, but ca. 40% of the oxide oxygen of NO remains unaccounted for by product isolation. This is due to some loss of the catalyst and oxidation of the CH_2Cl_2 solvent during turnover. Oxidation of solvent results in the gradual exchange of the SbF_6^- axial ligand for Cl^-. Product formation on reaction of NO with $(TPPC_2cap)Fe^{III}SbF_6$ can be approximated by the first-order rate law. Since the observed first-order rate constants at a given $[NO]_i$ are a linear function of the iron(III) porphyrin, the reaction is first order in this catalyst and essentially so in NO. However, the finding that the initial rates are independent of $[NO]_i$ establishes that the iron(III) porphyrin catalyst is saturated with NO on initiation of the reaction. The exchange of Cl^- for SbF_6^- axial ligand and some loss of catalyst during turnovers are responsible for the reactions changing from initial zero order to essentially first order in $[NO]_i$. Trapping of the intermediate ($(^{+\bullet}TPPC_2cap)Fe^{IV}O$) by 2,4,6-tri-*tert*-butylphenol (TBPH), 2,3-dimethyl-2-butene (TME), and *p*-cyano-*N*-methylaniline (MA) prevents solvent oxidation and porphyrin oxidative destruction. Under these trapping conditions the reaction is rapid and zero order in NO to completion. That the zero-order kinetics are due to saturation of the $[(TPPC_2cap)Fe^{III}]^+$ catalysts by NO was established by following the time course of the reaction in the Soret and Q spectral regions. The products with TME are TME epoxide (100%) and DA (100%) while with TBPH the radical TBP$^\bullet$ (100%) and DA (100%) are formed. The rate is also increased, but to a lesser extent, when using the poorer substrates, cyclohexene and norbornylene. These substrates also impart a zero-orderness to the appearance of products. The kinetics for the reaction of $(TPPC_2cap)Fe^{III}SbF_6$ with NO using TME, TBPH, and MA as substrates have been computer simulated with the requirement of steady-state saturation in the intermediate $(TPPC_2cap)Fe^{III}ON$. For successful simulations it is required that both the formation of $(^{+\bullet}TPPC_2cap)Fe^{IV}O$ + DA from $(TPPC_2cap)Fe^{III}ON$ and the reaction of $(^{+\bullet}TPPC_2cap)Fe^{IV}O$ with substrates (i.e., TME, TBPH, and MA) are partially rate limiting. At concentrations of added alkene less than that required for trapping of $(^{+\bullet}TPPC_2cap)Fe^{IV}O$ there are obtained, by cycloaddition of DA$^\bullet$ radical and alkene, tetrahydroquinoline derivatives.

In previous papers we have described kinetic and mechanistic studies dealing with the use of *p*-cyano-*N*,*N*-dimethylaniline *N*-oxide (NO) as an oxygen-transfer agent to a number of iron(III),[1] manganese(III),[2] and chromium(III)[3] porphyrins in the oxidation of N,N-disubstituted and N-monosubstituted anilines, 1-phenyl-1,2-ethanediol, and a variety of electron-acceptor traps as well as the epoxidation of a variety of alkenes. The reaction of NO with (*meso*-tetraphenylporphinato)iron(III) chloride[1c] ($(TPP)Fe^{III}Cl$), (*meso*-tetra(2,6-dichlorophenyl)porphinato)iron(III) chloride[1d] ($(Cl_8TPP)Fe^{III}Cl$), and (*meso*-tetra(2,6-dimethylphenyl)porphinato)iron(III) chloride[1e] ($(Me_8TPP)Fe^{III}Cl$) involves rate-determining transfer of oxygen from N → Fe as shown by the trapping of the $(^{+\bullet}Porph)Fe^{IV}O$ species. The product of the trapping experiments, aside from oxidized trap, is *p*-cyano-*N*,*N*-dimethylaniline (DA). Because the formation of $(^{+\bullet}Porph)Fe^{IV}O$ species is rate determining, its structure cannot be determined by use of NO as the oxygen-transfer agent.

(1) (a) Shannon, P.; Bruice, T. C. *J. Am. Chem. Soc.* **1981**, *103*, 4500. (b) Nee, M. W.; Bruice, T. C. *Ibid.* **1982**, *104*, 6123. (c) Dicken, C. M.; Lu, F.-L.; Nee, M. W.; Bruice, T. C. *Ibid.* **1985**, *107*, 5776. (d) Dicken, C. M.; Woon, T.-C.; Bruice, T. C. *Ibid.* **1986**, *108*, 1636. (e) Woon, T.-C.; Dicken, C. M.; Bruice, T. C. *J. Am. Chem. Soc.* **1986**, *108*, 7990.

(2) Powell, M. F.; Pai, E. F.; Bruice, T. C. *J. Am. Chem. Soc.* **1984**, *106*, 3277.

(3) (a) Yuan, L.-C.; Bruice, T. C. *J. Am. Chem. Soc.* **1985**, *107*, 512. (b) Yuan, L.-C.; Calderwood, T. S.; Bruice, T. C. *Ibid.* **1985**, *107*, 8273.

0002-7863/87/1509-3436$01.50/0 © 1987 American Chemical Society

However, it has been established (by controlled-potential spectroelectrochemistry at −70 °C) that 2e⁻ oxidation of a number of hydroxy ligated iron(III) porphyrins provides iron(IV)–oxo porphyrin π-cation radical products.[4] The addition of an oxygen atom to an iron(III) porphyrin is equivalent to the 2e⁻ oxidation of an iron(III) porphyrin ligated to hydroxide (eq 1). It is assumed, therefore, that (⁺•Porph)Fe^{IV}O species are formed on oxygen transfer from NO to iron(III) porphyrins.

$$(\text{Porph})\text{Fe}^{III}\text{OH} \xrightarrow[-H^+]{-2e^-} (^{+\bullet}\text{Porph})\text{Fe}^{IV}\text{O} \xleftarrow[-Cl^-]{-DA} (\text{Porph})\text{Fe}^{III}\text{Cl} + \text{NO} \quad (1)$$

The present study involves the reaction of NO with the antimony hexafluoride salt of the iron(III) C_2cap porphyrin described by Baldwin.[5] In undertaking this study we had two goals in mind. The first was to determine if a pentacoordinated iron(IV)–oxo porphyrin π-cation radical could be generated by oxygen transfer. The structure of the C_2cap porphyrin[6] is such that the SbF_6^-

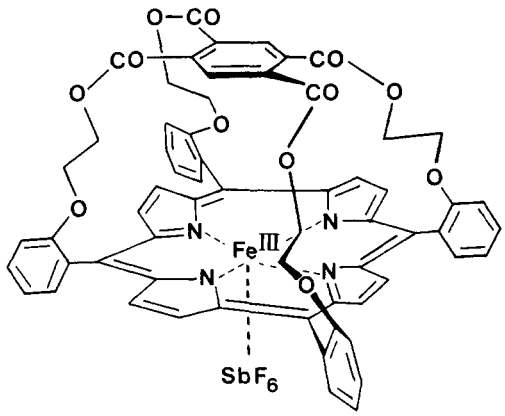

(TPPC$_2$cap)Fe^{III}SbF$_6$

counterion,[7] the *N*-oxide, and the oxidation products DA, *p*-cyano-*N*-methylaniline (MA), *N*-formyl-*p*-cyano-*N*-methylaniline (FA), *N,N'*-dimethyl-*N,N'*-bis(*p*-cyanophenyl)hydrazine (H), *N,N'*-bis(*p*-cyanophenyl)-*N*-methylmethylenediamine (MD), and *p*-cyanoaniline (A) are excluded from the capped face of the porphyrin ring. Our second objective was to ascertain if, by use of the weakly ligating SbF_6^- ligand and with the backside protection of the capped structure, it would be possible to realize saturation of the iron(III) porphyrin with NO. In doing so, the rate of catalyst turnover would be greatly increased and substrate oxidation by (⁺•TPPC$_2$cap)Fe^{IV}O might then be at least partially rate determining.

Experimental Section

C_2-capped (*meso*-tetraphenylporphinato)iron(III) chloride ((TPPC$_2$cap)Fe^{III}Cl) was prepared by the method of Baldwin et al.[5] and found to be identical with the previously reported material by UV–vis spectra. C_2-capped (*meso*-tetraphenylporphinato)iron(III) antimony(V) hexafluoride ((TPPC$_2$cap)Fe^{III}SbF$_6$) was prepared by modification of the method of Valentine.[7] (TPPC$_2$cap)Fe^{III}Cl (142.7 mg, 0.13 mmol) and $AgSbF_6$ (45.2 mg, 0.13 mmol) were refluxed in dry toluene (150 mL) for 4 h under a dry and oxygen-free atmosphere. Upon cooling, the precipitate was filtered and dried (N_2 glove box). The solid was washed with CH_2Cl_2 and the resulting solution filtered and evaporated *in vacuo* to yield the desired (TPPC$_2$cap)Fe^{III}SbF$_6$. The crude product was recrystallized from CH_2Cl_2/petroleum ether and was identified by its UV–vis spectra: λ_{max} (ε, 10^{-3} cm^{-1} M^{-1}) 400 (84.3), 517 (8.60), 580 (6.05), 630 nm (3.63). It was also identified by laser-desorbance Fourier transform mass spectrometry: *m/z* (M$^+$ − SbF$_6^-$) 1091.

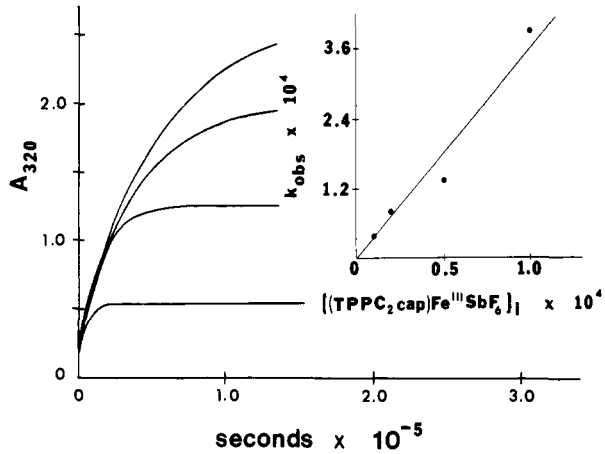

Figure 1. Plots of A_{320} vs. time for the (TPPC$_2$cap)Fe^{III}SbF$_6$-catalyzed decomposition of NO (where [(TPPC$_2$cap)Fe^{III}SbF$_6$]$_i$ = 8.9 × 10^{-5} M and [NO]$_i$ was varied from 7.7 × 10^{-4} to 5.4 × 10^{-3} M) showing that the initial rates are independent of the [NO]$_i$. The linear dependence of k_{obsd} on [(TPPC$_2$cap)Fe^{III}SbF$_6$]$_i$ is shown in the inset.

The μ-oxo dimer ((TPPC$_2$cap)Fe^{III})$_2$O can be identified spectrophotometrically by its characteristic Soret absorbance λ_{max} at 418 nm and a prominent β-band at 572 nm. *p*-Cyano-*N,N*-dimethylaniline *N*-oxide (NO) was prepared as described previously.[1c] *N,N'*-Di-*p*-cyanoazobenzene (AZ) was prepared according to the method of Ashley.[8] 6-Cyano-3,3,4,4-tetramethyl-*N*-methyl-1,2,3,4-tetrahydroquinoline (PQ) was obtained from preparative TLC (alumina, 70:30 hexane/$CHCl_3$, two elutions) of the reaction mixture resulting from the (TPPC$_2$cap)Fe^{III}SbF$_6$ (5.01 mg, 3.78 μmol) catalyzed decomposition of NO (34.1 mg, 210 μmol) in the presence of 0.1 M TME and was identified by ^{1}H NMR and high-resolution mass spectrometry: ^{1}H NMR ($CDCl_3$) δ 0.89 (s, 6 H), 1.17 (s, 6 H), 2.98 (s, 3 H), 3.09 (s, 2 H), 6.47 (d, 1 H, *J* = 3 Hz), 7.31 (d, 1 H, *J* = 3 Hz), 7.40 (s, 1 H); high-resolution mass spectrum, *m/z* 228.1616 (M$^+$, calcd for $C_{15}H_{20}N_2$ 228.1628); visible spectrum λ_{max} 304 nm (ε 1.2 × 10^4 M^{-1} cm^{-1}).

6-Cyano-3,4-norbornyl-*N*-methyl-1,2,3,4-tetrahydroquinoline (NPQ) was obtained from HPLC (see ref 1c) of the reaction mixture resulting from the (TPPC$_2$cap)Fe^{III}SbF$_6$ (5.01 mg, 3.78 μmol) catalyzed decomposition of NO (34.1 mg, 210 μmol) in the presence of 1.0 M norbornylene and was identified by ^{1}H NMR and high-resolution mass spectrometry: ^{1}H NMR ($CDCl_3$) δ 0.89–1.75 (complex m, 6 H), 2.13 (m, 1 H), 2.19 (m, 1 H), 2.36 (m, 1 H), 2.68 (d, 1 H, *J* = 9 Hz), 2.79 (dd, 1 H, *J* = 6, 12 Hz), 2.84 (s, 3 H), 3.10 (dd, 1 H, *J* = 6, 12 Hz), 6.61 (m, 1 H), 7.35 (m, 1 H), 7.41 (br s, 1 H); high-resolution mass spectrum, *m/z* 238.1462 (M$^+$, calcd for $C_{16}H_{18}N_2$ 238.1471). Cyclohexane and pentane were purified in the following manner: The alkane was washed with concentrated H_2SO_4 (3×) followed by H_2O (3×), dried over $CaCl_2$, and distilled from fresh $CaCl_2$ under a N_2 atmosphere. The sources of all other chemicals used in this study have been described previously.[1c] Kinetic studies were carried out in CH_2Cl_2 which was of the highest purity (described in a previous publication as Grade A[1c]) at 25 °C under an O_2-free and dry N_2 atmosphere. Conditions employed for HPLC and GC analyses have been described previously.[1c] The electrochemical techniques employed have been reported in a previous publication.[4] Spectra and extinction coefficients of DA oxidation products have been previously reported.[1c]

Results

The reaction of C_2-capped (*meso*-tetraphenylporphinato)iron(III) antimony(V) hexafluoride ((TPPC$_2$cap)Fe^{III}SbF$_6$) with *p*-cyano-*N,N*-dimethylaniline *N*-oxide (NO) yields *p*-cyano-*N,N*-dimethylaniline (DA), *p*-cyano-*N*-methylaniline (MA), *p*-cyanoaniline (A), *N*-formyl-*p*-cyano-*N*-methylaniline (FA), and *N,N'*-dimethyl-*N,N'*-bis(*p*-cyanophenyl)hydrazine (H). HPLC analysis of the reaction mixture at 280 and 320 nm gives complete material balance in amine products but does not account for all of the oxygen available from NO. For example, a typical reaction yields 68% DA, 12% MA, 1% A, 6% FA, and 7% H. In addition to the aniline products, formaldehyde is produced in ~3% yield

(4) (a) Lee, W. A.; Calderwood, T. S.; Bruice, T. C. *Proc. Natl. Acad. Sci. U.S.A.* **1985**, *82*, 4301. (b) Calderwood, T. S.; Lee, W. A.; Bruice, T. C. *J. Am. Chem. Soc.* **1985**, *107*, 8272. (c) Calderwood, T. S.; Bruice, T. C. *Inorg. Chem.* **1986**, *25*, 3789.

(5) Almog, J.; Baldwin, J. E.; Crossley, M. J.; Debernardis, J. F.; Dyer, R. L.; Huff, J. R.; Peters, M. K. *Tetrahedron* **1981**, *37*, 3589.

(6) (a) Jameson, G. B.; Ibers, J. A. *J. Am. Chem. Soc.* **1980**, *102*, 2823. (b) Sabat, M.; Ibers, J. A. *Ibid.* **1982**, *104*, 3715.

(7) (a) Quinn, R.; Nappa, M.; Valentine, J. S. *J. Am. Chem. Soc.* **1982**, *104*, 2588. (b) Shelly, K.; Bartczak, T.; Scheidt, W. R.; Reed, C. A. *Inorg. Chem.* **1985**, *24*, 4325.

(8) Ashley, J. B.; Berg, S. S. *J. Chem. Soc.* **1957**, 3089.

Table I. Percentage Yield of Products for the Decomposition of NO (2.6×10^{-3} M) Catalyzed by $(TPPC_2cap)Fe^{III}SbF_6$ (7.5×10^{-5} M) in the Presence of Varying $[TME]_i$

$[TME]_i$, M	percentage yield						total yield, %	TME oxide, %
	DA	MA	A	H	FA	PQ		
1.0	92	3	0	0	5	0	100	96
0.10	57	<1	0	2	4	36	99	54
0.01	51	1	0	1	3	37	93	11
0.0	66	16	0	8	6	0	96	0

(based on the method of Nash[9]). Thus, approximately 40% of the oxygen derived from NO is unaccounted for. Increase in A_{320} (Figure 1) is due mainly to the formation of DA while H and MA also contribute, and the plots of A_{320} vs. time can be approximated by the first-order rate law. Under the conditions of $[NO]_i \gg [(TPPC_2cap)Fe^{III}SbF_6]_i$ and at constant iron(III) porphyrin concentration, the overall rate of the reaction decreases as $[NO]_i$ is increased. However, as evident from Figure 1, above an NO concentration of $\sim 7.7 \times 10^{-4}$ M the initial rates stay the same regardless of $[NO]_i$. At constant $[NO]_i$ the apparent pseudo-first-order rate constant, k_{obsd}, shows a linear dependence on the $[(TPPC_2cap)Fe^{III}SbF_6]_i$ catalyst (inset to Figure 1). Thus, under the pseudo-first-order condition of $[NO]_i \gg [catalyst]_i$, the rate of reaction decreases with increase in turnover number, regardless of whether it is changed by altering the initial concentration of the porphyrin or the initial concentration of the *N*-oxide. In other words, the fewer the turnovers, the greater the pseudo-first-order rate constant (k_{obsd}) for the formation of products at 320 nm. The change from initial zero-order to first-order dependence upon $[NO]_i$ and the decrease in k_{obsd} with increase in $[NO]_i$ is due to (i) oxidation of CH_2Cl_2 solvent with production of Cl^-, which in turn becomes the axial ligand in place of SbF_6^-, and (ii) oxidative destruction of the $TPPC_2cap$ moiety. The oxygen imbalance between NO used and detectable products is accounted for, in some part, by these two oxidations. The change of ligation of $(TPPC_2cap)Fe^{III}SbF_6$ on reaction with NO was investigated by spectral scanning during the reaction. The observed change, for all reactions investigated, in axial ligand from SbF_6^- to Cl^- is characterized by a bathochromic shift in the Soret band from 400 to 421 nm. Also, from the absorbance at 421 nm it was found that between 5% and 20% of the porphyrin, depending on turnover number, was missing.

The reaction of $(TPPC_2cap)Fe^{III}Cl$ (8.8×10^{-5} M) and NO was followed spectrophotometrically at 320 nm for 10 turnovers ($[NO]_i = 8.9 \times 10^{-4}$ M) and 30 turnovers ($[NO]_i = 2.7 \times 10^{-3}$ M). The product distribution was essentially the same as seen when $(TPPC_2cap)Fe^{III}SbF_6$ was the catalyst. Likewise, the percent yields of the products were independent of $[NO]_i$. The reactions followed pseudo-first-order kinetics, and unlike the results with $(TPPC_2cap)Fe^{III}SbF_6$, initial rates were found to be dependent upon NO concentration. The pseudo-first-order rate constants decreased with increasing $[NO]_i$ in a manner analogous to the $(TPPC_2cap)Fe^{III}SbF_6$-catalyzed decomposition of NO. The latter observation is to be explained by some catalyst oxidative destruction. The pseudo-first-order rate constants for the product appearance with $(TPPC_2cap)Fe^{III}Cl$ were much slower than those seen with $(TPPC_2cap)Fe^{III}SbF_6$ ($k_{obsd} = 3.2 \times 10^{-5}$ s^{-1} for 10 turnovers and $k_{obsd} = 7.4 \times 10^{-6}$ s^{-1} for 30 turnovers for the $(TPPC_2cap)Fe^{III}Cl$-catalyzed decomposition of NO while $k_{obsd} = 3.6 \times 10^{-4}$ s^{-1} for 10 turnovers and $k_{obsd} = 5.3 \times 10^{-5}$ s^{-1} for 30 turnovers for the $(TPPC_2cap)Fe^{III}SbF_6$-catalyzed decomposition of NO).

The time course for the formation of each product in the $(TPPC_2cap)Fe^{III}SbF_6$ (9.0×10^{-5} M) catalyzed decomposition of NO (2.6×10^{-3} M) was followed under nitrogen (see Experimental Section ref 1c). The first-order rate constants for appearances of DA (2.2×10^{-5} s^{-1}), H (5.4×10^{-5} s^{-1}), FA (6.3×10^{-5} s^{-1}), and A (3.5×10^{-5} s^{-1}) are comparable while the formation of MA exhibits a pronounced lag phase (vide infra).

(9) Nash, T. *Biochem. J.* **1953**, *55*, 416.

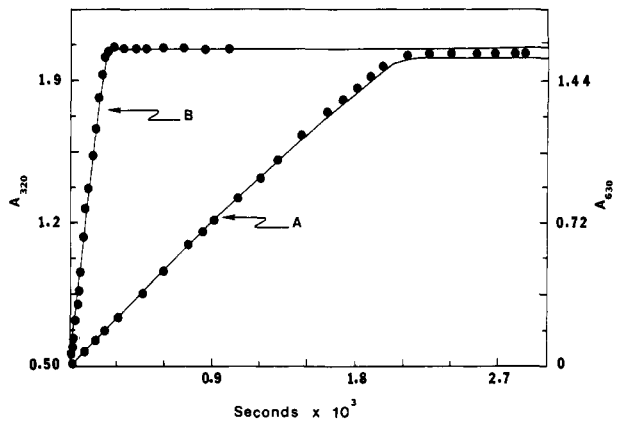

Figure 2. (A) Experimental points for the appearance of DA with time as monitored at 320 nm which accompanies the reaction of $(TPPC_2cap)Fe^{III}SbF_6$ (7.5×10^{-5} M) and NO (2.6×10^{-3} M) in the presence of 1.0 M TME. The lines which correlate the experimental points have been computer generated by simulation using the reactions of Scheme I and the rate constants given in the Discussion. (B) Experimental points for the spectral time course for the oxidation of TBPH monitored at 630 nm (λ_{max} for TBP$^{\bullet}$) where $[NO]_i = 2.0 \times 10^{-3}$ M, $[(TPPC_2cap)Fe^{III}SbF_6]_i = 6.7 \times 10^{-5}$ M, and $[TBPH]_i = 0.30$ M. The experimental points have been fitted with computer-generated lines employing the reactions of Scheme I and the rate constants given in the Discussion.

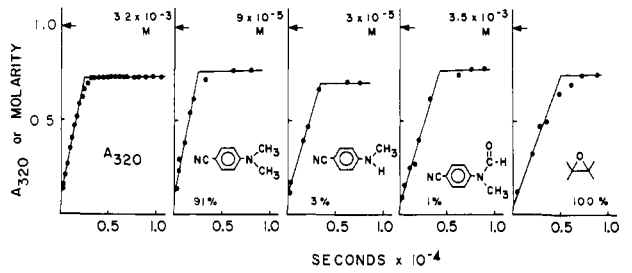

Figure 3. Plots of A_{320} vs. time and the time courses (determined by HPLC and GC) for the products that are formed (DA, MA, and FA, and TME oxide) in zero-order processes in the $(TPPC_2cap)Fe^{III}SbF_6$ (7.5×10^{-5} M) catalyzed decomposition of NO (2.6×10^{-3} M) in the presence of 1.0 M TME.

The reaction of NO and $(TPPC_2cap)Fe^{III}SbF_6$ in the presence of different concentrations of 2,3-dimethyl-2-butene (TME) was monitored spectrophotometrically at 320 nm. Product analysis by HPLC and GC was carried out at termination of the reaction (Table I). Examination of Table I shows that with an increase in $[TME]_i$ there is an increase in the percent yield of DA and TME oxide and a decrease in the percent yield of the other products (based on $[NO]_i$). This is due to the preferential reaction of the $(^{+\bullet}TPPC_2cap)Fe^{IV}O$ species with the alkene. It should be noted that in intermediate concentrations of TME an additional product is obtained—6-cyano-3,3,4,4-tetramethyl-*N*-methyl-1,2,3,4-tetrahydroquinoline (PQ)—that results from the cycloaddition of the radical DA$^{\bullet}$ with TME (see Discussion section for all details). When all $(^{+\bullet}TPPC_2cap)Fe^{IV}O$ is trapped by TME, PQ is not formed, and DA and TME oxide are the sole products (100% yield based on $[NO]_i$).

The time course for reaction of NO (2.6×10^{-3} M) with $(TPPC_2cap)Fe^{III}SbF_6$ (7.5×10^{-5} M) in the presence of TME at 0.1 M was monitored at 320 nm while aliquots were withdrawn with time and subjected to HPLC analysis at 280 and 320 nm. The formations of DA, H, and FA are first order, with rate constants of 8.5×10^{-5}, 1.2×10^{-4}, and 1.1×10^{-4} s^{-1}, respectively. Thus, the rates of product formation are increased by about 2-fold in the presence of 0.1 M TME. The appearance of MA with time is found to be multiphasic. The product PQ arises abruptly after a prolonged lag phase of $\sim 1.4 \times 10^4$ s. In the presence of 1.0 M TME, the formation of DA is very rapid (increase in A_{320}; Figure 2A) and the formation of both DA and TME oxide with

time zero order to completion (Figure 3). Above a TME concentration of 0.10 M, no oxygen imbalance is observed.

The reaction of NO (2.0×10^{-3} M) and (TPPC$_2$cap)Fe^{III}SbF$_6$ (6.7×10^{-5} M) in the presence of 2,4,6-tri-*tert*-butylphenol (TBPH) was followed at 630 nm (λ_{max} of the radical oxidation product TBP$^{\bullet}$, ϵ_{630} 400 M^{-1} cm^{-1}). As $[TBPH]_i$ is increased, the appearance of TBP$^{\bullet}$ with time gradually changes from first order to zero order. At 0.3 M TBPH, the formation of TBP$^{\bullet}$ is zero order to completion of the reaction (Figure 2B). The yield of DA is 100% and there is no oxygen loss (Table II), and at 0.3 M TBPH, much as TME at 1.0 M, all higher valent iron–oxo species are trapped. Spectral scanning establishes that there is not exchange of SbF_6^- for Cl^- ligand. However, even though $[NO]_i$ and $[(TPPC_2cap)Fe^{III}SbF_6]_i$ are essentially the same in both experiments, the TBPH reaction comes to an abrupt completion in 4–5 min whereas the TME experiment comes to an abrupt completion in 30–35 min.

The ability of the iron(IV) porphyrin π-cation radical species (resulting from oxygen transfer from NO to the (TPPC$_2$cap)Fe^{III}SbF$_6$) to oxidize the products of NO decomposition (DA, MA, FA, and H—each at initial concentrations of $\sim 1.0 \times 10^{-3}$ M) was investigated. The computation of the percentage yields in Table III was carried out in the following manner: For DA, FA, and H the yields were calculated after subtraction of the added reagent and are based upon $[NO]_i$. When MA is added, the percentage yields of products, based upon $[NO]_i$, add up to more than 100%. Addition of MA gives an increase in the yield of DA and H and a decrease in the yield of FA. This is so because DA is spared at the expense of MA oxidation and the product of DA oxidation is FA whereas MA oxidation yields only H. On addition of DA there is observed a small increase in the yields of F and H and no change in the first-order rate of disappearance of NO. Also, addition of DA provides complete nitrogen balance in products. The percent yield of products formed on decomposition of NO is not influenced by the addition of H or FA, and there is seen to be losses of accountability for 30% and 33% of oxygen derived from NO, respectively. In contrast, addition of MA provides a drastic increase in the rate of product formation (A_{320} vs. time). With addition of MA the time course possesses more zero-order character, much as seen for those kinetic runs where TME and TBPH are oxidizable substrates. When the reaction is carried out at an $[MA]_i = 4.3 \times 10^{-3}$ M, the reaction is zero order to completion (Figure 4).

Reaction of NO (2.5×10^{-3} M) with (TPPC$_2$cap)Fe^{III}SbF$_6$ (9.8×10^{-5} M) in the Presence of 1.0 M Cyclohexene or Norbornylene. With cyclohexene the plot of A_{320} vs. time exhibits the characteristics of mixed zero- and first-order kinetics (Figure 5). Neither cyclohexene nor norbornylene are capable of completely trapping the higher valent iron–oxo porphyrin species so that the acceleration of rate is not comparable to that obtained on addition of TBPH, TME, or MA. For the cyclohexane experiment, the yield of epoxide was 52% while the aniline products obtained and their yields were DA, 95%; MA, 4%; and H, 3%. Once again, an oxygen loss ($\sim$30–35%) was encountered. When norbornylene was employed as a substrate, the epoxide was obtained in 44% while DA and H were obtained in 80% and 9%, respectively. An additional product was also seen and upon its isolation by HPLC and characterization by ^{1}H NMR and high-resolution MS was found to be the 6-cyano-3,4-norbornyl-*N*-methyl-1,2,3,4-tetrahydroquinoline (NPQ) resulting from the cycloaddition of DA$^{\bullet}$ to norbornylene (see Discussion Section). Again, an oxygen imbalance of 30–35% was obtained.

Exchange of SbF_6^- Ligand by Cl^- and Loss of Catalysis due to Oxidative Destruction of the Porphyrin in the Presence of Oxidizable Substrates. Change of ligation of (TPPC$_2$cap)Fe^{III}SbF$_6$ on reaction with NO in the presence of added oxidizable substrates was investigated by spectral scanning before and after each kinetic study. In the experiments with added DA a considerable portion of the iron(III) porphyrin undergoes axial-ligand exchange of Cl^- for SbF_6^-. With TME at 1.0 M there is no ligand exchange. Most interesting is the observation that at low concentrations of TME (0.01M), not only has a small amount of the (TPPC$_2$cap)Fe^{III}Cl been formed but the μ-oxo dimer $[(TPPC_2cap)Fe^{III}]_2O$ is also present. Much the same was found in the experiments employing 1.0 M norbornylene or 4.3×10^{-3} M MA.

Table II. Effect of $[TBPH]_i$ on the Product Yields in the Decomposition of NO (2.0×10^{-3} M) Catalyzed by (TPPC$_2$cap)Fe^{III}SbF$_6$ (6.7×10^{-5} M)

	percentage yield		
$[TBPH]_i$, M	DA	MA	TBP$^{\bullet}$
0.30	100	2	100
0.20	95	3	96
0.10	92	4	94
0.02	90	6	90

Table III. Effect of the Presence of the Oxidation Products at Time Zero on the Yields of Products in the (TPPC$_2$cap)Fe^{III}SbF$_6$ (7.5×10^{-5} M) Catalyzed Decomposition of NO (1.8×10^{-3} M)

oxidation product added	initial concentration, M	percentage yield			
		DA	MA	H	FA
		68	12	7	6
DA	9.9×10^{-4}	60	16	15	10
MA	1.1×10^{-3}	89	15	31	0
H	8.2×10^{-4}	66	15	9	5
FA	1.3×10^{-3}	74	13	10	7

Addition of Nonsubstrate Hydrocarbons Has an Accelerating Effect on the Rate of Reaction of NO with (TPPC$_2$cap)Fe^{III}SbF$_6$. In the presence of the nonsubstrates, cyclohexane and pentane (at 1.0 M), the rate of reaction of NO (2.7×10^{-3} M) with (TPPC$_2$cap)Fe^{III}SbF$_6$ (9.1×10^{-5} M) is increased as much as seen with cyclohexene (Figure 6). As in the experiment with 1.0 M cyclohexene, the plots of ΔA_{320} with time take on considerable zero-order character. However, the presence of cyclohexane or pentane does not alter the products nor their yields: i.e., DA, 68%; MA, 12%; A, 1%; FA, 6%; H, 7%; and an oxygen imbalance of $\sim$40%. This observation establishes that the rate enhancements brought about by these hydrocarbons is not due to an impurity which is oxidized by the intermediate ($^{+\bullet}$TPPC$_2$cap)Fe^{IV}O. Addition of benzene (1.0 M) has only a small effect upon the rate and products, and their yields remain unaltered. For the reactions in the presence of cyclohexane, pentane, or benzene (all at 1.0 M), remaining porphyrin exists almost exclusively as the Cl^- ligated iron(III) C$_2$cap porphyrin at the completion of the reaction.

Establishment of the Condition of Saturation of Iron(III) Porphyrin with NO. Repetitive spectral scanning of Soret (350–500-nm) and Q (700–500-nm) bands upon rapid mixing of solutions of (TPPC$_2$cap)Fe^{III}SbF$_6$ (7.0×10^{-5} M) and NO (3.10×10^{-3} M) in the presence of TME (1.0 M) were carried out. At the Q band, there was observed an immediate increase in absorbance (ϵ_{max} 8.6×10^3 to 1.15×10^4) at 514 nm and a corresponding shift of λ_{max} = 580–590 nm and λ_{max} = 630–645 nm. After a period of 25 min, the spectrum reverts back to its original form with a slight shift of λ_{max} = 514–517 nm. This result shows that in the presence of TME (which being easily oxidized prevents the oxidation of solvent and generation of Cl^-), the easily displaced SbF_6^- axial ligand is instantly (on the time scale of the experiment) exchanged by NO and that as the NO is consumed ligation by SbF_6^- is reestablished. The lifetime of the NO ligated species ((TPPC$_2$cap)Fe^{III}ON) corresponds reasonably well to the time of completion of the zero-order reaction ($\sim$30 min). Only a slight increase in absorbance at the Soret band (400 nm) was observed on the mixing of components. No new absorbance band appeared hypsochromic to the original Soret peak.

Redox potentials of (TPPC$_2$cap)Fe^{III}Cl were determined by cyclic voltammetry and controlled-potential oxidation and reduction in CH_2Cl_2 at 25 °C. The CV exhibited single anodic and cathodic waves separated at their peaks by 100 mV with a midpoint potential of +1.14 V (SCE). Controlled-potential oxidation established the involvement of one electron. The absorption spectrum of the product of the controlled-potential oxidation at +1.14 V exhibited an absorbance maximum for the Soret band

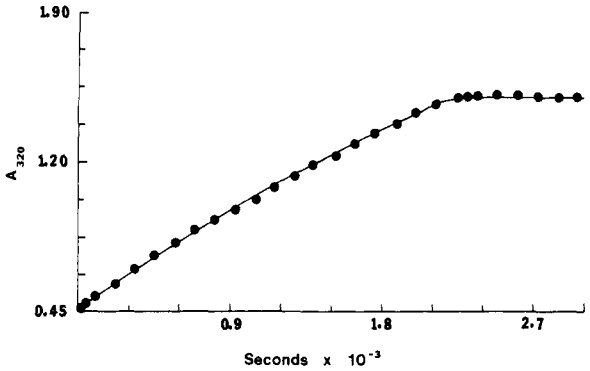

Figure 4. Plot of A_{320} vs. time showing the effect of the addition of MA (4.3×10^{-3} M) on the kinetics of the decomposition of NO (1.8×10^{-3} M) catalyzed by $(TPPC_2cap)Fe^{III}SbF_6$ (7.5×10^{-5} M).

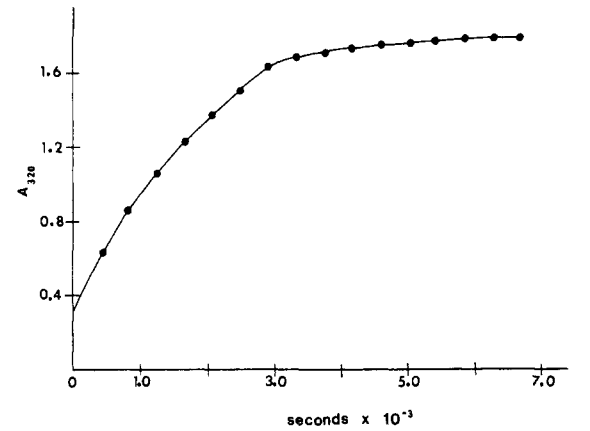

Figure 5. Plot of A_{320} vs. time for the $(TPPC_2cap)Fe^{III}SbF_6$ (9.80×10^{-5} M) catalyzed decomposition of NO (2.50×10^{-3} M) in the presence of 1.0 M cyclohexene.

at 376 nm as well as weaker absorbance peaks at approximately 520, 550, and 600 nm. The spectrum of the one electron oxidized species is much as expected for an iron(III) porphyrin π-cation radical.[10] A CV of this product showed anodic and cathodic peaks separated by 110 mV with a midpoint potential at +1.05 V. The difference of 90 mV for the CV midpoint potentials for $(TPPC_2cap)Fe^{III}Cl$ and the corresponding π-cation radical tells us that the oxidation product obtained in the rapid time frame (100 mV s^{-1}) of CV oxidation (total CV in ca. 30 s) is different from that obtained by the slow controlled-potential oxidation (20 min to completion). This process is reversible. Thus, controlled-potential reduction of the product required one electron to generate a species indistinguishable by its spectrum from $(TPPC_2cap)Fe^{III}Cl$. The potential associated with $2e^-$ oxidation of $(TPPC_2cap)Fe^{III}Cl$ exceeds +1.70 V and could not be determined due to solvent oxidation.

The potential for the formation of the iron(III) porphyrin π-cation radical $(^{+\bullet}TPPC_2cap)Fe^{III}Cl$ is 100 mV less positive than that for the formation of $(^{+\bullet}TPP)Fe^{III}Cl$. Previous work in this laboratory[4] has shown that the oxidation potentials for formation of chloro-ligated iron(III) porphyrin π-cation radicals and their iron(IV)–oxo porphyrin π-cation radicals are identical. This suggests that the oxidation potential for formation of $(^{+\bullet}TPPC_2cap)Fe^{IV}O$ is also 100 mV less positive than the corresponding potential for formation of $(^{+\bullet}TPP)(Cl)Fe^{IV}O$. Therefore, oxidation of the aniline products DA and MA by $(^{+\bullet}TPPC_2cap)Fe^{IV}O$ should not occur as readily as their oxidation by $(^{+\bullet}TPP)(Cl)Fe^{IV}O$. This feature could spare $(^{+\bullet}TPPC_2cap)Fe^{IV}O$ so that it reacts with the CH_2Cl_2 solvent while $(^{+\bullet}TPP)(Cl)Fe^{IV}O$ does not.

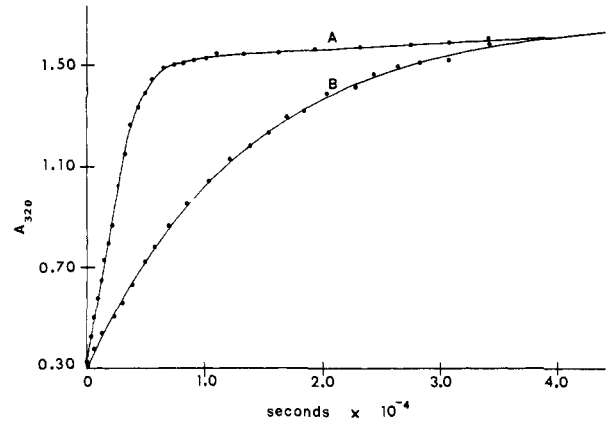

Figure 6. Plots of A_{320} vs. time for the $(TPPC_2cap)Fe^{III}SbF_6$ (9.1×10^{-5} M) catalyzed decomposition of NO (2.7×10^{-3} M) in the presence of 1.0 M pentane (A) and in its absence (B), showing the effect of the nonsubstrate hydrocarbon on the kinetics of the reaction of $(TPPC_2cap)Fe^{III}SbF_6$ and NO.

Discussion

Reaction of C_2-Capped (*meso*-Tetraphenylporphinato)iron(III) Antimony(V) Hexafluoride ($(TPPC_2cap)Fe^{III}SbF_6$) with *p*-Cyano-*N*,*N*-dimethylaniline *N*-Oxide (NO) in the Absence of Added Reagents (CH_2Cl_2 at 25 °C). To summarize the conclusion which may be reached from experiments without added oxidizable substrates: (i) The reaction of $(TPPC_2cap)Fe^{III}SbF_6$ with NO provides, with the exception of MD, the same products as seen with $(TPP)Fe^{III}Cl$. Formation of DA, A, FA, and H follows the first-order rate law whereas the formation of MA exhibits a pronounced lag phase.

(ii) At the various concentrations of the $(TPPC_2cap)Fe^{III}SbF_6$ and NO employed, material balance in all nitrogen-containing products is found. However, ~40% of the oxygen atoms derived from NO remain unaccounted for. This marks the first instance of porphyrin oxidation when employing NO as an oxygen-transfer agent. Oxidation of the porphyrin is not a property of its capped structure but is due to the fact that four phenyl substituents at the meso position possess ortho alkoxide substituents. In unpublished work we have found that (tetrakis(4-methoxyphenyl)porphinato)iron(III) chloride also undergoes partial oxidative destruction on reaction with NO.[11]

(iii) Oxidation of CH_2Cl_2 solvent by the intermediate $(^{+\bullet}TPPC_2cap)Fe^{IV}O$ provides Cl^- which slows the reaction appreciably by exchanging with SbF_6^- as ligand. Solvent oxidation and oxidative destruction of the porphyrin differentiate the present system from those which involve the reaction of NO with $((TPP)Fe^{III}Cl)$,[1c] $((Cl_8TPP)Fe^{III}Cl)$,[1d] and $((Me_8TPP)Fe^{III}Cl)$.[1e] Due to the loss of porphyrin and the exchange of SbF_6^- axial ligand for Cl^-, the reaction is slowed on continual turnover of the catalyst. The reaction of $(TPPC_2cap)Fe^{III}Cl$ with NO has been determined to be first order in both *N*-oxide and catalyst, and the pseudo-first-order rate constants are more than 10-fold slower than when employing $(TPPC_2cap)Fe^{III}SbF_6$. (Due to the ligand exchange during turnover with $(TPPC_2cap)Fe^{III}SbF_6$, the actual rate constant for this species must, therefore, be much greater than 10 times the rate constant for $(TPPC_2cap)Fe^{III}Cl$.) With the more electron deficient $(TPP)Fe^{III}Cl$,[1c] $(Cl_8TPP)Fe^{III}Cl$,[1d] and $(Me_8TPP)Fe^{III}Cl$[1e] the higher valent iron–oxo porphyrin π-cation radical is quenched by oxidation of DA and MA or by oxidation of added oxidizable substrates. Apparently, the less positive potential (100 mV) for the formation of $(^{+\bullet}TPPC_2cap)Fe^{IV}O$, as compared to $(^{+\bullet}TPP)Fe^{IV}O$, decreases the reactivity of this species with the immediate products DA and MA more so than its reaction with the CH_2Cl_2 solvent.

(iv) Oxidation of solvent at the expense of DA, MA, etc. ox-

(10) Phillippi, M. A.; Goff, H. M *J. Am. Chem. Soc.* **1982**, *104*, 6026.

(11) Dicken, C. M.; Bruice, T. C., unpublished results.

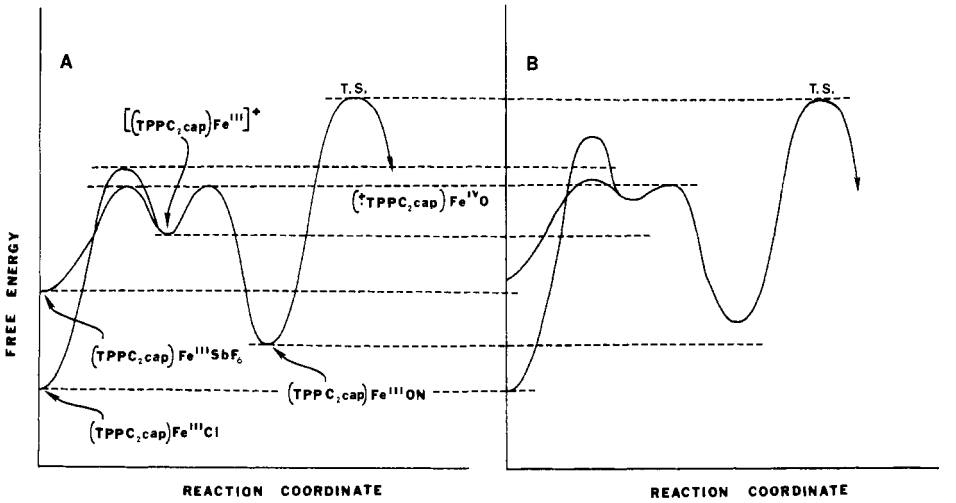

Figure 7. Reaction coordinate cartoons which may be used to explain the positive kinetic solvent effect on the rate of turnover reaction of $(TPPC_2cap)Fe^{III}SbF_6$ with NO. Plot A provides a comparison of the reaction coordinates when reactions are initiated with $(TPPC_2cap)Fe^{III}SbF_6$ and $(TPPC_2cap)Fe^{III}Cl$. The plot accommodates saturation of iron(III) porphyrin by NO when the axial ligand is SbF_6^- and the sharing of the common intermediate $[(TPPC_2cap)Fe^{III}]^+$, $(TPPC_2cap)Fe^{III}ON$, and the transition state (T.S.). Plot B depicts rational changes in the free energy contents of intermediates (relative to T.S. and $(TPPC_2cap)Fe^{III}Cl$) which might be expected on changing the solvent from the polar CH_2Cl_2 to the less polar 1 M alkane in CH_2Cl_2.

idation results in percent yields and ratios of aniline products which are different than seen when using $(TPP)Fe^{III}Cl$ as catalyst. More DA is present than seen when $(TPP)Fe^{III}Cl$ is the catalyst, and, thus, less MA is available for further oxidations leading to A, H, and MD.

(v) Initial rates establish that the turnover of the $(TPPC_2cap)Fe^{III}SbF_6$ catalyst involves saturation of this moiety by NO—a result which is not too surprising since the SbF_6^- ligand was chosen on the basis of its very weak association with the iron(III) moiety.[7]

(vi) Since neither NO nor SbF_6^- is of sufficiently small dimension[12] to fit under the cap structure of the porphyrin, the iron moiety of the iron(IV)–oxo porphyrin π-cation radical, formed on oxygen transfer from NO, is most likely pentacoordinate at least during the initial turnovers.

Solvent Effect brought about by Addition of Hydrocarbons. The addition of cyclohexane and pentane (to 1.0 M) to a solution containing NO and $(TPPC_2cap)Fe^{III}SbF_6$ changes the kinetics of turnover catalysis from first order to almost zero order in NO (Figure 6) while benzene (1.0 M) has only a slight positive effect on the rate. The rate enhancements are not due to the presence of oxidizable impurities in the alkane samples since the presence of cyclohexane or pentane does not influence the yields of DA, MA, A, FA, and H nor the oxygen imbalance or ligand exchange of Cl^- for SbF_6^-. The "positive kinetic solvent effect" is characteristic of the presence of SbF_6^- as axial ligand. Thus, the first-order rates of reaction of NO with $(TPPC_2cap)Fe^{III}Cl$ and $(TPP)Fe^{III}Cl$ in CH_2Cl_2 are not changed by the presence of 1.0 M cyclohexane. With $(TPPC_2cap)Fe^{III}Cl$ we find that the products and their yields are unaltered by addition of 1.0 M cyclohexane (with the exception of the formation of 1.0% cyclohexanol, based upon $[NO]_i$).[1c]

The nature of the C_2-capped porphyrin structure dictates that axial ligand exchange occurs by a dissociative mechanism (eq 2). The observations that the solvent effect is not associated with change in the nature of the products nor their yields but is characterized by an enhancement in rate and a change in kinetics

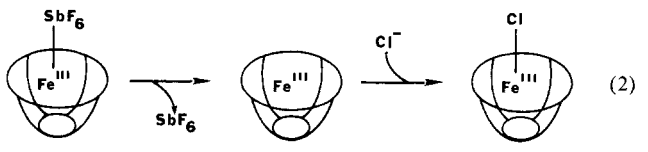

(2)

from pseudo-first-order to partially zero order can only mean that ligation of Cl^- is inhibited when the polarity of the solvent is decreased. A decrease in the rate of formation of $(TPPC_2cap)Fe^{III}Cl$, without changing the rate of formation of Cl^- by solvent oxidation, would prolong the time that the iron(III) porphyrin remains saturated with NO. This, in turn, would impart a zero-order character to the reaction kinetics and increase the rate of catalyst turnover. The cartoon of Figure 7A compares the reactions of $(TPPC_2cap)Fe^{III}SbF_6$ and $(TPPC_2cap)Fe^{III}Cl$ with NO. These two reactions involve the common intermediates $[(TPPC_2cap)Fe^{III}]^+$ and $(TPPC_2cap)Fe^{III}ON$ and also the common transition state for the formation of $(^{+\bullet}TPPC_2cap)Fe^{IV}O$. Since the reaction involving $(TPPC_2cap)Fe^{III}SbF_6$ involves saturation of catalyst by NO, while that involving $(TPPC_2cap)Fe^{III}Cl$ does not, the free energy content of the former must be substantially greater than that of the latter. These features represent the critical aspects of Figure 7A. Chloride ion formed on oxidation of solvent can compete with NO and SbF_6^- for $[(TPPC_2cap)Fe^{III}]^+$. Inspection of Figure 7A shows that the ligation of Cl^- is exergonic when compared to the formation of $(TPPC_2cap)Fe^{III}ON$ and particularly $(TPPC_2cap)Fe^{III}SbF_6$. In order to slow the rate of Cl^- ligation to $[(TPPC_2cap)Fe^{III}]^+$ the free energy barrier for this reaction must be raised relative to that for reaction of NO and SbF_6^- with $[(TPPC_2cap)Fe^{III}]^+$. In the cartoon of Figure 7B the standard-state free energies have been raised, relative to the free energy contents of $(TPPC_2cap)Fe^{III}ON$ and T.S., according to their polarity (i.e., $[(TPPC_2cap)Fe^{III}]^+ > (TPPC_2cap)Fe^{III}ON^+ > (TPPC_2cap)Fe^{III\delta+}SbF_6^{\delta-} \sim$ transition state for Cl^- ligation with $[(TPPC_2cap)Fe^{III}]^+$). Comparison of the cartoons of Figure 7A and 7B shows that such an assumption could be argued to give the required slowing down of the formation of $(TPPC_2cap)Fe^{III}Cl$ on reaction of $(TPPC_2cap)Fe^{III}SbF_6$ with NO in a solvent made less polar by addition of a hydrocarbon. The cartoons of Figure 7A and 7B exaggerate the changes in relative free energies that would be required. There is no claim to uniqueness in the rationale for the solvent effect, but it is deemed as reasonable.

The rate enhancement upon addition of 1 M cyclohexene or norbornylene as well as the change in kinetics toward zero order in $[NO]_i$ is about the same as that seen with cyclohexane and pentane. With these hydrocarbons one would anticipate a solvent effect as seen with the alkanes. With cyclohexene and norbornylene there is obtained the epoxides in 52% and 44% yields, respectively. The alkenes serve as moderately good substrates, but in their presence there is still an oxygen imbalance in the products and solvent oxidation as shown by exchange of Cl^- for SbF_6^- ligand.

(12) Passmore, J.; Taylor, P.; Whidden, T.; White, P. S. *Can. J. Chem.* **1979**, *57*, 968.

Table IV. Rate Constants Employed (Units in s and M) for the Fitting of the Reactions of Scheme I to the Zero-Order Appearance of *p*-Cyano-*N*,*N*-dimethylaniline (DA) with Assumption of Saturation in $(TPPC_2cap)Fe^{III}ON$

	substrates		
rate constants	TME	TBPH	MA
k_a/k_{-a}	5.0×10^{-5}	5.0×10^{-5}	5.0×10^{-5}
k_a	$>1 \times 10^2$	$>1 \times 10^2$	$>1 \times 10^2$
k_{-a}	$<2 \times 10^6$	$<2 \times 10^6$	$<2 \times 10^6$
k_b/k_{-b}	$>6 \times 10^5$	$>6 \times 10^5$	$>6 \times 10^5$
k_b	$>6 \times 10^5$	$>6 \times 10^5$	$>6 \times 10^5$
k_{-b}	1.0	1.0	1.0
k_c/k_{-c}	4.0×10^{-4}	4.0×10^{-4}	4.2×10^{-4}
k_c	2.0×10^{-2}	1.5×10^{-1}	1.7×10^{-2}
k_{-c}	5.0×10	3.6×10^2	4.0×10
k_d	4.5×10^{-1}		
k_e or $k_{e'}$		2.0×10	7.0×10
k_f or $k_{f'}$		2.0×10	7.0×10

When DA is used as an oxidizable substrate (8.8×10^{-4} M) there is observed those changes of product yields expected for DA oxidation. The pseudo-first-order rate constant for product formation is not, however, altered. This lack of influence of addition of DA on the kinetics when combined with the observations that addition of MA and TBPH provide large rate enhancements and change the reaction from first to zero order in product formation support a reversible oxygen-transfer reaction. If $(^{+\bullet}TPPC_2cap)Fe^{IV}O$ reacts with DA in both the forward and reverse directions (eq 3) there is not to be anticipated a change

$$((TPPC_2cap)Fe^{III})^+ + NO \rightleftarrows (TPPC_2cap)Fe^{III}ON \rightleftarrows (^{+\bullet}TPPC_2cap)Fe^{IV}O + DA \quad (3)$$

$$(^{+\bullet}TPPC_2cap)Fe^{IV}O + DA \rightarrow (TPPC_2cap)Fe^{III} + CH_2O + MA, \text{ etc.}$$

in the rate of catalyst turnover on addition of DA to the reaction solution. This is so because the partition coefficient for $(^{+\bullet}TPPC_2cap)Fe^{IV}O$ is not altered. A back-reaction of DA with $(^{+\bullet}TPPC_2cap)Fe^{IV}O$ requires that product (DA) oxidation is partially rate determining.

Compounds 2,3-Dimethyl-2-butene (TME), 2,4,6-Tri-*tert*-butylphenol (TBPH), and *p*-Cyano-*N*-methylaniline (MA) Are of Particular Interest as Substrates. When MA is used as a substrate at but 4.3×10^{-3} M there is a profound increase in rate, and the reaction is zero order in [NO] to completion (figure 4). That MA addition results in zero-order dependence upon [NO] to completion is in accord with the finding of complete oxygen balance in the products in the presence of MA and lack of both SbF_6^- ligand exchange by Cl^- and porphyrin oxidation.

At 1.0 M TME or 0.30 M TBPH, it is found that trapping of the higher valent iron–oxo porphyrin species is complete. This is shown by the following observations: (i) DA is the only aniline product, and it is formed in 100% yield. (ii) Based on the initial concentrations of NO, epoxidation of TME occurs in 100% yield as does oxidation of TBPH to TBP•. (iii) There is complete material balance without oxygen loss. (iv) There is absolutely no detectable exchange of the SbF_6^- ligand for a Cl^- ligand. (v) The formation of DA with time is seen to be completely zero order as one would anticipate for a reaction in which the catalyst is saturated in substrate and where there is no product inhibition nor catalyst destruction. In the presence of TME or TBPH, the reaction is not only changed from first to zero order, but turnover of the catalyst and consumption of NO are profoundly enhanced. The described characteristics of the reactions are dependent upon the SbF_6^- ligand rather than the $[(TPPC_2cap)Fe^{III}]^+$ moiety. No such rate enhancements are seen in the presence of TBPH on reaction of NO with $(TPP)Fe^{III}Cl$ or $(TPPC_2cap)Fe^{III}Cl$.[13]

At 1.0 M TME it has been possible to observe spectrally the change of SbF_6^- axial ligation of the porphyrin by NO as a function of time. These experiments (Results) show that the SbF_6^- ligand exchanges with NO immediately on mixing solutions of $(TPPC_2cap)Fe^{III}SbF_6$ and NO. The initial spectrum of $(TPPC_2cap)Fe^{III}SbF_6$ is recovered virtually unchanged at the time of the abrupt completion of the reaction. These results support saturation of the catlayst with NO and unimolecular decay of the complex to form $(^{+\bullet}TPPC_2cap)Fe^{IV}O$ and DA.

If oxygen transfer from N → Fe were rate limiting and the only roles played by TME, TBPH, and MA were as traps for the $(^{+\bullet}TPPC_2cap)Fe^{IV}O$ species, then the zero-order rate constants determined with these reagents would be identical. The observation is that the zero-order rate constants differ appreciably. A partial explanation is found in the study of DA oxidation from which one can infer substrate oxidation to be partially rate controlling.[14] Scheme I accommodates the above experimental observations. Computer fitting of Scheme I to the experimental

Scheme I

$$(TPPC_2cap)Fe^{III}SbF_6 \underset{k_{-a}}{\overset{k_a}{\rightleftharpoons}} [(TPPC_2cap)Fe^{III}]^+ + SbF_6^-$$

$$[(TPPC_2cap)Fe^{III}]^+ + NO \underset{k_{-b}}{\overset{k_b}{\rightleftharpoons}} (TPPC_2cap)Fe^{III}ON$$

$$(TPPC_2cap)Fe^{III}ON \underset{k_{-c}}{\overset{k_c}{\rightleftharpoons}} (^{+\bullet}TPPC_2cap)Fe^{IV}O + DA$$

$$(^{+\bullet}TPPC_2cap)Fe^{IV}O + TME \xrightarrow{k_d} [(TPPC_2cap)Fe^{III}]^+ + \text{TME oxide}$$

$$(^{+\bullet}TPPC_2cap)Fe^{IV}O + TBPH \xrightarrow{k_e} [(TPPC_2cap)Fe^{IV}OH]^+ + TBP^\bullet$$

$$[(TPPC_2cap)Fe^{IV}OH]^+ + TBPH \xrightarrow{k_f} [(TPPC_2cap)Fe^{III}]^+ + TBP^\bullet + H_2O$$

$$(^{+\bullet}TPPC_2cap)Fe^{IV}O + MA \xrightarrow{k_{e'}} [(TPPC_2cap)Fe^{IV}OH]^+ + MA^\bullet$$

$$[(TPPC_2cap)Fe^{IV}OH]^+ + MA \xrightarrow{k_{f'}} [(TPPC_2cap)Fe^{III}]^+ + MA^\bullet + H_2O$$

points which represent the change in A_{320} due to the formation of DA is shown in Figure 2. The points in Figures 2 and 4 represent experimental results whereas the lines are computer generated from Scheme I. The computer fitting was made with the assumption that $k_a/k_{-a} = 5.0 \times 10^{-5}$ M, $k_b/k_{-b} = 6.0 \times 10^5$ M^{-1}, and $k_c/k_{-c} = 4.0 \times 10^{-4}$ M for all three substrates, TBPH, TME, and MA, and that the partially rate-controlling substrate oxidation steps change in rate constants according to the respective reactivity of the substrates. The various rate constants used in the simulation are given in Table IV. The rate constants k_a and k_{-a} represent minimal and maximal values, respectively. The rate constant k_b represents the minimal value. The constants k_a, k_{-a}, k_b, and k_{-b} were chosen in such a way that the ratios k_a/k_{-a} and k_b/k_{-b} give a favorable saturated equilibrium formation of the $(TPPC_2cap)Fe^{III}ON$ species. The rate constants for oxygen transfer within the $(TPPC_2cap)Fe^{III}ON$ complex and the reversible oxygen transfer from $(^{+\bullet}TPPC_2cap)Fe^{IV}O$ to DA have been altered for different substrates to give good fitting. However, the ratio of two rate constants (k_c/k_{-c}) is constant for all three substrates, implying that the ΔG° for the oxygen-transfer step is substrate independent while $\Delta G^\ddagger$ is dependent (but only within 1.0 kcal M^{-1}) upon the nature of the substrate. The rate constants k_d, k_e, k_f, $k_{e'}$, and $k_{f'}$ for the oxidation of substrates were chosen by iteration and found to be specific for each substrate. In the reaction of

(13) Ostovic, D.; Bruice, T. C., unpublished results.

(14) Collman, J. P.; Brauman, J. I.; Meunier, B.; Hayashi, T.; Kodadek, T.; Raybuck, S. A. *J. Am. Chem. Soc.* **1985**, *107*, 2000.

Scheme II

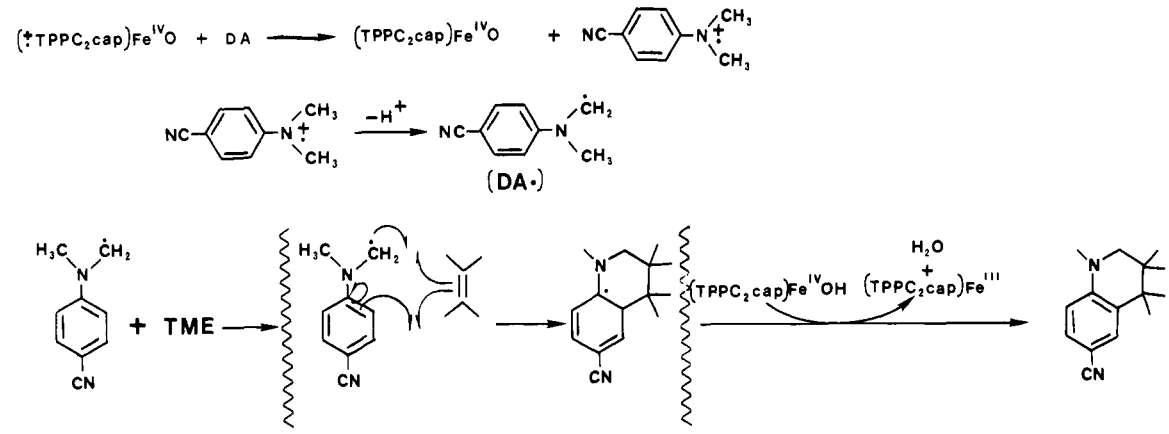

TBPH and MA with iron–oxo species, k_f and $k_{f'}$ were chosen to be equal to k_e and $k_{e'}$. The rate constant for $1e^-$ oxidation of MA by ($^{+\bullet}$TPPC$_2$cap)Fe^{IV}O of 70 M^{-1} s^{-1} may be compared to that of 300 M^{-1} s^{-1} calculated for ($^{+\bullet}$TPP)Fe^{IV}O oxidation of MA.[1c] This comparison is most reasonable since the $1e^-$ oxidation potential for the formation of ($^{+\bullet}$TPPC$_2$cap)Fe^{IV}O. The magnitude of these rate constants is also reasonable. The $1e^-$ oxidation potential for conversion of MA to MA$^\bullet$ is +1.45 V.[1c] Neither DA nor MA is oxidizable by horseradish peroxidase.[15,16] From the $1e^-$ oxidation potentials for MA → MA$^\bullet$, the approximated potential (see Results) for (TPPC$_2$cap)Fe^{IV}O → ($^{+\bullet}$TPPC$_2$cap)-Fe^{IV}O of +1.14 V and the computed forward rate constant of 70 M^{-1} s^{-1} for the oxidation of MA by ($^{+\bullet}$TPPC$_2$cap)Fe^{IV}O, it can be calculated that (i) the standard free energy for the equilibrium MA + ($^{+\bullet}$TPPC$_2$cap)Fe^{IV}O ⇄ MA$^\bullet$ + (TPPC$_2$cap)Fe^{IV}O is endergonic by ~7 kcal M^{-1} and (ii) the rate of the oxidative reaction (TPPC$_2$cap)Fe^{IV}O + MA$^\bullet$ → ($^{+\bullet}$TPPC$_2$cap)Fe^{IV}O + MA is ~10^7 M^{-1} s^{-1}.

Scheme I will also fit the kinetic data for the oxidation of TME, TBPH, and MA, if it is assumed that there is saturation kinetics with respect to ($^{+\bullet}$TPPC$_2$cap)Fe^{IV}O species (reaction k_c/k_{-c}). Therefore, there are two kinetically identical types of fittings of Scheme I to the experimental data (i.e., saturation in (TPPC$_2$cap)Fe^{III}ON vs. saturation in ($^{+\bullet}$TPPC$_2$cap)Fe^{IV}O). Repetitive spectral scanning of the reaction mixture has been carried out with TME at 1.0 M. This experiment shows that there is an increase in absorbance of the Q band at 514 nm immediately after adding NO to the reaction mixture containing (TPPC$_2$cap)Fe^{III}SbF$_6$ and TME. This absorbance decays with respect to time to its original position. The sharp increase in absorbance is not due to the formation of ($^{+\bullet}$TPPC$_2$cap)Fe^{IV}O as the principal iron–porphyrin species in solution. This is shown by the observation that the porphyrin Soret band does not undergo a hypsochromic shift upon addition of NO—an expectation for the conversion of the porphyrin moiety to a π-cation radical.[4] The only reasonable mechanism involves saturation of the catalyst by NO. Proanalysis of the computer-generated data for concentrations of various species reveals that the catalyst is saturated with respect to NO in the course of the reaction.

A Most Interesting Aspect of This Study Has Been the Discovery of the Formation of Tetrahydroquinolines in the Reaction of NO with (TPPC$_2$cap)Fe^{III}SbF$_6$ in the Presence of Alkenes. At 0.01 and 0.10 M (but not higher) concentrations of TME (with $[NO]_i$ = 2.6 × 10^{-3} M and $[(TPPC_2cap)Fe^{III}SbF_6]_i$ = 7.5 × 10^{-5} M) and at 1.0 M norbornylene ($[NO]_i$ = 2.5 × 10^{-3} M and $[(TPPC_2cap)Fe^{III}SbF_6]_i$ = 9.8 × 10^{-5} M) the products 6-cyano-3,3,4,4-tetramethyl-*N*-methyl-1,2,3,4-tetrahydroquinoline (PQ) and 6-cyano-3,4-norbornyl-N-methyl-1,2,3,4-tetrahydroquinoline (NPQ) were obtained in ~36% and ~15% yields based on $[NO]_i$,

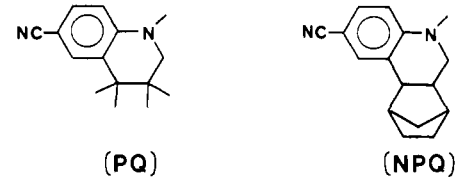

(PQ) (NPQ)

respectively. We propose that PQ and NPQ are formed via radical cycloadditions that involve the intermediate *p*-cyano-*N*,*N*-dimethylaniline radical formed after one-electron transfer from DA to ($^{+\bullet}$TPPC$_2$cap)Fe^{IV}O followed by proton transfer as shown in Scheme II. The lack of formation of the cycloaddition product (PQ) at higher TME concentrations is due to the trapping of the higher valent iron–oxo porphyrin π-cation species by TME to yield DA and TME oxide in 100% yield. Under this trapping condition DA is not oxidized to DA$^\bullet$. Cycloaddition reactions involving amine radical species and alkenes have been studied by Swan and co-workers.[17]

Acknowledgment. This work was supported by grants from the National Institutes of Health and the American Cancer Society.

(15) Galliani, G.; Rindone, B.; Marchesini, A. *J. Chem. Soc., Perkin Trans. 1* **1978**, 456.
(16) Galliani, G.; Rindone, B. *Bioorg. Chem.* **1981**, *10*, 283.
(17) (a) Roy, R. B.; Swan, G. A. *J. Chem. Soc., Chem. Commun.* **1968**, 1446. (b) Swan, G. A., *Ibid.* **1969**, 20. (c) Roy, R. B.; Swan, G. A. *J. Chem. Soc. C* **1969**, 1886.